Published by
NIGERIAN SOCIETY OF PHYSICAL SCIENCES
Available online @ https://journal.nsps.org.ng/index.php/jnsps

J. Nig. Soc. Phys. Sci. 7 (2025) 2376

Journal of the Nigerian Society of Physical Sciences

Patti formation shales at Agbaja Plateau: A geochemical window into the provenance and tectonic setting history of the Southern Bida Basin, Nigeria

Olusola J. Ojo[a,*], Suraju A. Adepoju[b], Ayodeji Awe[a], Kehinde A. Alalade[a]

[a]*Department of Geology, Federal University, P.M.B. 373, Oye Ekiti, Nigeria*
[b]*Department of Geology and Mineral Science, Kwara State University, P.M.B. 1530, Malete, Kwara State, Nigeria*

Abstract

Agbaja Plateau is one of the mesas that dotted the topography of north centrally located Bida Basin. Seventeen shale samples from the exposed Maastrichtian Patti Formation at Agbaja Plateau were analyzed using x-ray fluorescence (XRF) and inductive coupled plasma mass spectrophotometry (ICPMS) with the aim of unroofing the provenance, weathering and paleotectonic history of the basin. The provenance-sensitive elemental ratios; Al_2O_3/TiO_2 , Cr/Ni, Th/Cr, La/Sc, Th/Sc and Th/Co and the binary diagrams of Al_2O_3 *vs* TiO_2, TiO_2 *vs* Zr, reveal that the shales originated from felsic source rock. The Light rare earth elements (LREE) enrichment, Flat heavy rare earth elements (HREE) model, a negative Eu anomaly and positive Ce anomalies, and La/Yb-REE bivariate diagram also reveal sediments derivation predominantly from felsic protolith. The plots of SiO_2 versus $K_2O/Na_2O$and Ti/Zr versus La/Sc, and Ti/Zr–La/Sc, Th-Sc-Zr/10, Th–Co-Zr/10, and La-Th-Sc discrimination diagrams show that the shales plotted in the passive margin. The Zr/Sc and Th/Sc ratios and low ICV values show first cycle recycling with heavy mineral enrichment. LREE, with flat HREE distributions, as well as the normalized Gd/Yb and La/Yb enrichment indicate similarity with the post-Archean Australian Average Shales (PAAS). The high values of chemical index of weathering, chemical index of alteration and Plagioclase Index of Alteration indicate that the protolith experienced strong chemical weathering. In conclusion, the study suggest that the investigated shales were derived mainly from felsic source rocks and deposited in passive margin setting similar to the adjacent sedimentary basins in Nigeria and west Africa.

DOI:10.46481/jnsps.2025.2376

Keywords: Shales, Geochemistry, Provenance, Bida, Patti

Article History :
Received: 21 September 2024
Received in revised form: 15 January 2024
Accepted for publication: 29 March 2025
Available online: 03 May 2025

Communicated by: O. J. Abimbola

1. Introduction

The Nigerian government's renewed focus on increasing petroleum reserves by exploring inland basins, including the Bida Basin, motivated this study. this present investigation. This paper focusses on the shale samples exposed at the Agbaja Plateau in the southern arm of the Bida Basin (Figure 1), central Nigeria. The Bida Basin was linked to Anambra Basin by the Trans-Saharan Seaway and their propagating line continued westward all the way to the Atlantic Ocean [1]. Several researchers have contributed to the unravelling of the geological dynamics that controlled and shaped the sedimentation style and the sedimentary fill in the Western and Central African

*Corresponding author Tel. No.: +234-803-503-6503.
Email address: olusola.ojo@fuoye.edu.ng (Olusola J. Ojo)

Rifts (WCARS) basins using paleoweathering, paleoclimatic, paleosalinity, paleoredox and paleoenvironmental conditions. Generally, the pioneer works on provenance research includes; Dickinson and Suczek [2], Bhatia [3], Bhatia [4], Dickinson *et al*. [5], Dypvik [6], Taylor and McLennan [7], Bhatia and Crook [8], Suttner and Dutta [9], Pettijohn *et al*. [10], McLennan [11], Dera *et al*. [12], McLennan *et al*. [13], Kroonenberg [14], Weltje *et al*. [15], Armstrong-Altrin *et al*. [16] and Armstrong-Altrin and Verma [17] underscore the critical role of geochemical tools in unraveling provenance, tectonic settings, and depositional environments, significantly advancing the fields of sedimentary and tectonic research. These studies have laid the groundwork for advancements in sedimentary and tectonic research, providing a solid foundation for this current study to build upon.

Some researchers have carried out studies related to the petrography and sedimentary geochemistry of sandstones from the Bida Basin for the purpose of determining the provenance of the sediments and the tectonic origin. Ojo *et al.* [18] described sandstones of the Patti Formation as dominantly quartzarenites and litharenite with minor arkosic form. Nton and Adamolekun [19] employed petrographic and geochemical studies of the outcropped sandstone of Patti Formation, and concluded that they are more mature than sandstones of Lokoja Formation. Bankole *et al*. [20] inferred highly immature sediments for the sandstones of Lokoja Sandstones, and more mature Patti Formation sandstones. Ojo *et al*. [21] described the Lokoja Formation sandstones as arkosic and that they were sourced dominantly from felsic rocks and passive margin setting.

The Agbaja Plateau is a prominent geological structure within the Southern Bida Basin, known for its ironstone deposits and stratigraphic significance. Recently, however, thick shales associated with coals were discovered interbedded below the ironstones at various part of the plateau. The newly discovered shales of the Patti Formation in this region offer a unique opportunity to investigate the geochemical characteristics that can reveal the provenance, depositional history, and tectonic processes that influenced the basin's development. To date, the geochemical composition of these shales and their significance for understanding the basin's origin and tectonic history remain unexplored. This approach is particularly significant, as shales represent a more comprehensive archive of geochemical, and paleoenvironmental due to their finer grain size and higher organic matter content. By examining the geochemical signatures and depositional conditions of these shales, this study will offer a more nuanced understanding of sediment provenance, paleoenvironmental dynamics, and organic matter enrichment within the Patti Formation. In this context, the study aims to provide a comprehensive geochemical analysis of the shales at the Agbaja Plateau, with the following objectives; to determine the paleotectonic setting of the Southern Bida Basin, to determine the protolith of the shales, to unravel the maturity and weathering history, and to compare the geochemical characteristics of the shales with other similar formations in the region and globally and placing the findings within a broader geological context. This novel emphasis will not only address gaps in the existing literature but also contributes to refining regional geological models and improving our understanding of Cretaceous sedimentary environments in West Africa.

2. Origin and geological settings

The southern Bida Basin is part of the larger structure, called Bida Basin. Different hypotheses have been put forward by several authors to explain its evolutionary history; King [22], Kennedy [23] and Adeleye [24] described the Bida Basin as a rift-bounded tensional structure produced by faulting associated with the Benue Trough system and drifting apart of the South American and African plate. Ojo and Ajakaiye [25] interpreted Landsat imageries and borehole log data and suggested that the basin is bounded by a system of linear faults trending Northwest-Southeast. Geophysical data by Kogbe *et al*. [26] and Ajakaiye and Burke [27] supported the rift model earlier proposed. Ref. [28] proposed that the Bida Basin evolved as a result of post-Santonian shallow cratonic sag while Ref. [29] suggested a wrench fault tectonic model for the origin of the Bida Basin. The gravity studies by Ojo [30] point to series of central positive anomalies flanked by negative anomalies, similar to the adjacent Benue Trough and typical of rift structures.

The stratigraphic chart of the Bida Basin is presented in Figure 2. The northern Bida Basin consists of the Bida Formation, Sakpe Formation, the Enagi Formation and the Batati Ironstone Formation whereas the Southern Bida Basin consists of the Lokoja Formation, the Patti Formation and the Agbaja Formation [31, 32]. In the southern Bida basin, the oldest unit is the Campanian Lokoja Formation and it is stratigraphically equivalent to the Bida Formation in the northern part of the Basin. It is succeeded by the Maastrichtian Patti Formation (the lateral equivalent of the Enagi Formation). The Agbaja Formation which is the lateral equivalent of the Batati Ironstone in the northern part of the Basin capped the entire sequence.

3. Methodology

3.1. Fieldwork and sampling

For this study, lithologic sequences of the Patti Formation, exposed along the Agbaja Plateau, were systematically sampled. GPS devices were used to record sample locations, and the coordinates were subsequently applied in map creation. The two lithological sections examined, consisting of sandstone, siltstone, shale, and coal, were measured, described, and sampled at appropriate intervals (Figure 3). Only shale samples were selected for analysis to align with the study's specific aims and objectives.

3.2. Sample preparation, and analytical techniques

In order to achieve the aim and objectives of this research, seventeen shale samples were selected for a whole rock inorganic geochemical analysis. This was done to determine the major oxides, trace and rare earth elements composition using X-ray fluorescence (XRF) and inductively coupled plasma mass spectrometry (ICPMS) analyses. Prior to the analysis at the MS Analytical Laboratory Canada,approximately 50–100 g of each

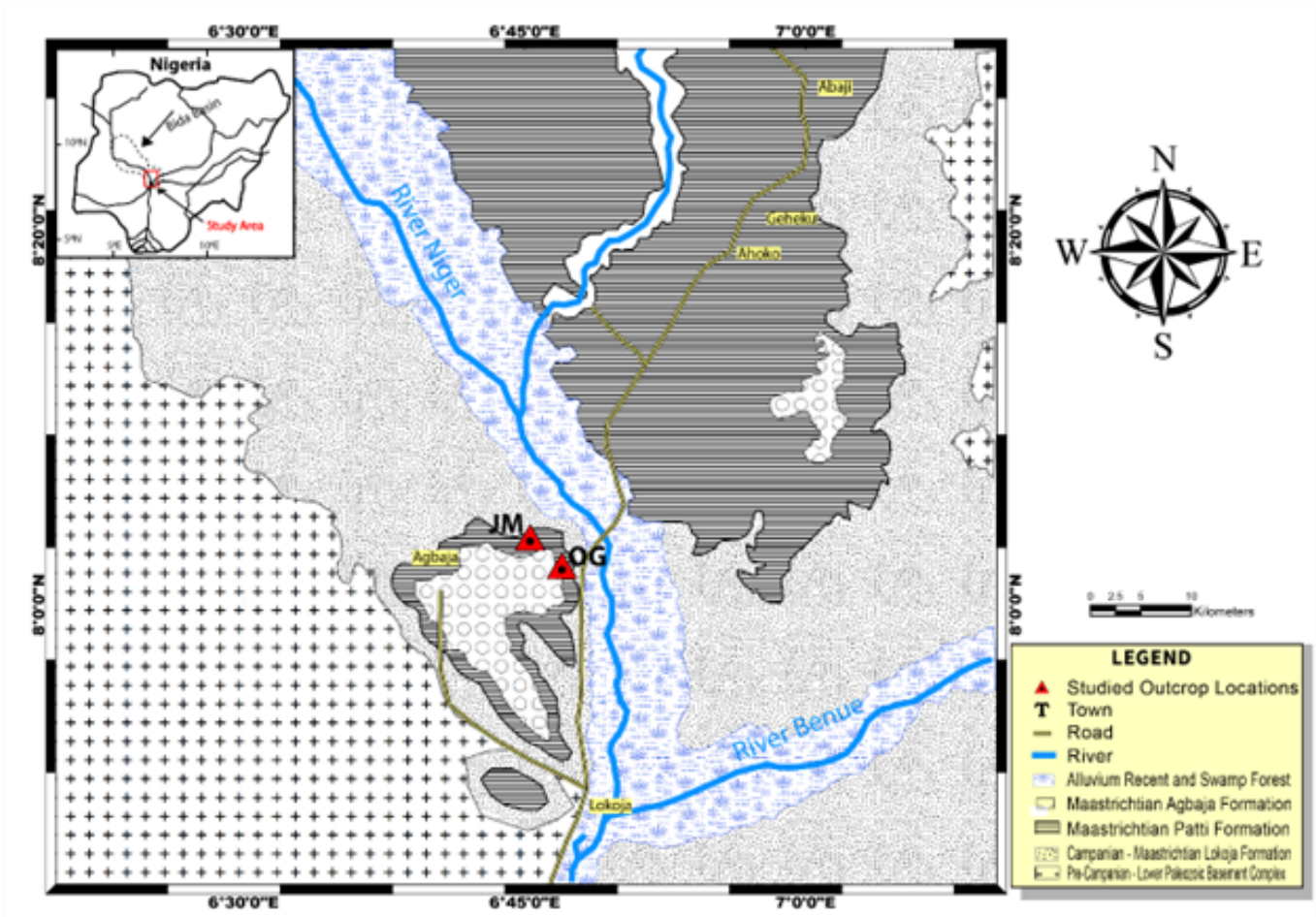

Figure 1. Map of Nigeria showing Bida Basin (Modified after [33]).

sample was reduced to 2–4 mm chips and pulverised using a mortar agate mill to prevent contamination.

For the XRF analysis, 0.20 g aliquot was weighed into a graphite crucible and it was mixed with 1.50 g of $LiBO_2/Li_2B_4O_7$ flux.The crucibles were heated at 980°C for 30 minutes, and the resulting bead was dissolved in 5% ACS-grade HNO3 diluted in deionised water. The major oxides data from each sample were generated and then recorded. Replicate analyses of the samples, conducted twice along with the associated standards used in the study, reveal an error margin of 1 to 2%.

To evaluate the trace and rare elements composition, 50.0 mg of each sample was digested with mixture of 3.0 ml of concentrated hydrogen fluoride (HF), 1.0 ml of concentrated hydrogen nitrate (HNO3) and 1.0 ml of concentrated hydrogen per chlorate ($HClO_4$) for 48 h in a tightly closed Teflon vessel on a hot plate at temperature <150 °C. Later, the solution was evaporated to dryness and extracted with 60.0 ml of 1% HNO_3. Each sample was run against a standard reference material (SRMs) viz., GSR 4, GSR 6, GXR-6 to correct long-term instrument drift. Accuracy of the trace and REE element analyses is within 5%.

4. Results

4.1. Major oxides

The bulk elemental composition the shale samples in form of major oxide, trace and rare earth elements and their calculated ratios are presented in Tables 1 to 3. Higher concentrations of major oxides (Tables 1 and 2) were recorded for SiO2 (2.64–79.65%; Avg. 53.31%), Al2O3 (0.95–23.80%; Avg. 12.78%), and Fe2O3 (1.12–24.51%; Avg. 6.21%). Other oxides showed lower concentrations; CaO (0.02-0.04%), MgO (0.03-0.32), Na_2O (0.01-0.15%), K_2O (0.02-1.07%), MnO (0.01-0.26%), TiO_2 (0.01-0.55), and P_2O_5 (0.10-1.74%).

4.2. Trace elements

For the trace elements, the relative abundance, average concentration, and calculated ratios, as detailed in Tables 3 and 4, were utilized in the binary and ternary plots to assess their geochemical patterns. The concentrations of these trace elements in the studied shale samples are consistently lower than the average values reported for the Upper Continental Crust (UCC) and Post-Archean Australian Shale (PAAS) as referenced by

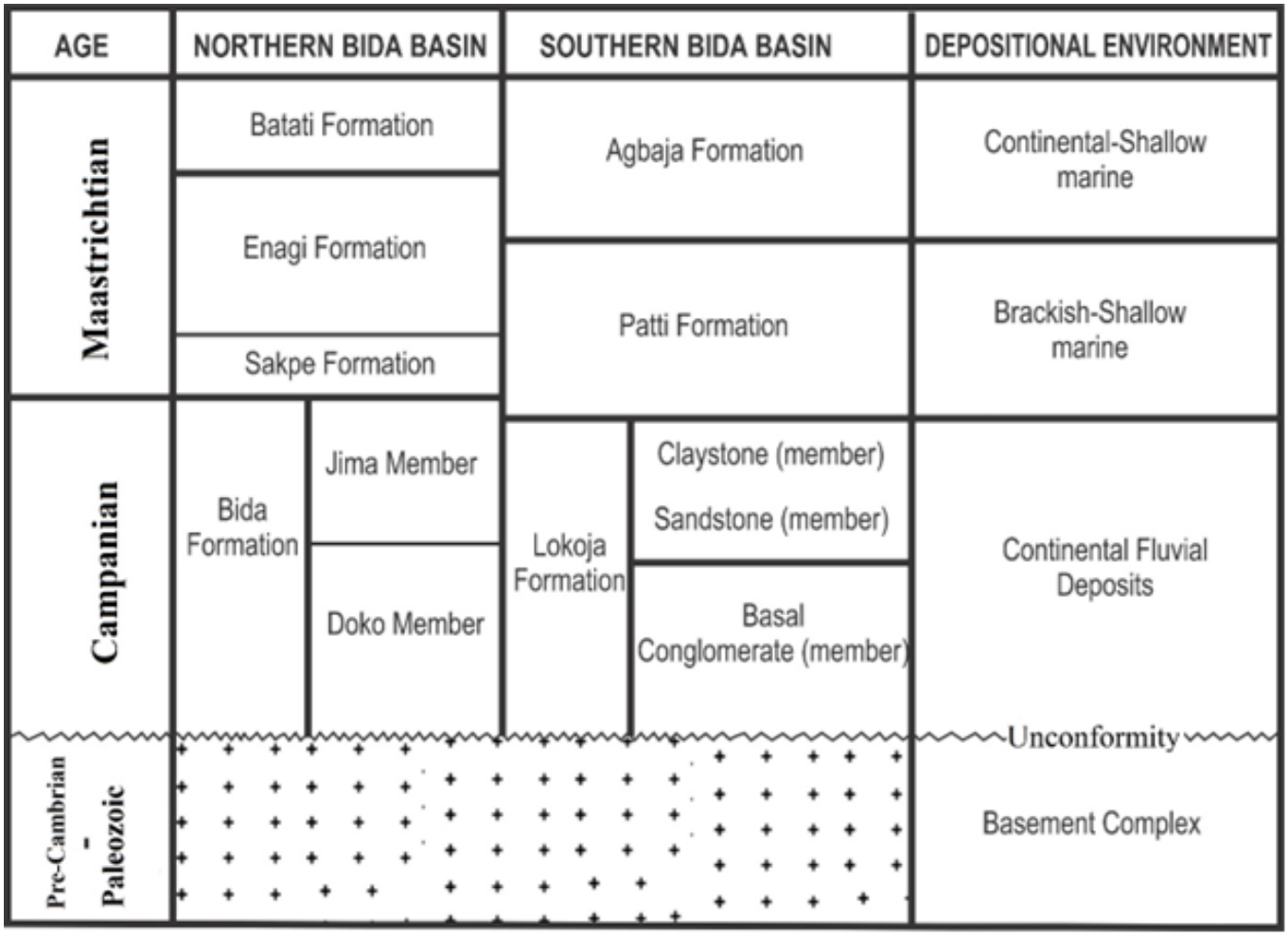

Figure 2. Stratigraphic framework of the Bida Basin (Adapted from [34]).

Ref. [35], suggesting that the shales may have experienced specific geochemical processes or sources distinct from the typical continental shale composition.

4.3. Rare earth elements

The concentrations of rare earth elements (REEs) in the analyzed shale samples range from 39.40 ppm to 1607.37 ppm (Table 5), indicating a wide variability in their distribution across the samples. The ratios of light rare earth elements (LREEs) to heavy rare earth elements (HREEs) range from 5.89 to 11.12, reflecting a general enrichment in LREEs. The Eu/Eu* ratio, which is a key indicator of redox conditions during sedimentation, varies between 0.41 and 0.69, suggesting moderate fractionation between Eu and other REEs, likely influenced by depositional environments. The Ce/Ce* ratio, ranging from 0.93 to 1.26, further supports this interpretation, indicating variations in the oxygenation conditions of the paleo environment. Other ratios, including $(La/Lu)_N$, $(La/Yb)_N$, and $(Gd/Yb)_N$, range from 4.64 to 11.99, 4.11 to 10.78, and 0.70 to 1.71 respectively, providing additional insights into the patterns of REE fractionation and the tectonic and depositional settings of the shales. These geochemical markers collectively enhance our understanding of the provenance and paleoclimatic conditions under which the shales were deposited.

5. Interpretation and discussion

5.1. Chemical maturity and weathering history

The chemical classification of the studied shales was attempted in order to evaluate the degree of their compositional maturity. From the submission of Rollinson [36], the contents of alkali (Na_2O+K_2O) constitute an important chemical maturity index and the values of their ratios are interpreted as follows; less than 2.0 indicates little or no feldspar contents which invariably signify high chemical maturity, while values greater than 2.0 indicate feldspar-rich which suggests low chemical maturity. The alkali content of the shale samples (0.03–1.20%; mean 0.63) reflects high chemical maturity. Potter [37] also submitted that ratio of SiO_2/Al_2O_3 in clastic rocks are sensitive to sediment recycling and weathering processes and hence useful as maturity indicator. According to Roser and Korsch [38]

Table 1. Major oxide composition of the Patti formation shales at Agbaja Plateau.

Sample	SiO_2	Al_2O_3	Fe_2O_3	CaO	MgO	Na_2O	K_2O	MnO	TiO_2	P_2O_5	LOI
JM1C	63.46	14.24	5.15	0.02	0.10	0.04	0.52	0.04	1.65	0.06	11.63
JM1D	50.72	8.60	10.94	0.02	0.06	0.10	0.51	0.06	1.23	0.04	23.7
JM1E	67.08	12.34	5.95	0.03	0.11	0.03	0.71	0.06	1.60	0.04	9.99
JM1H	59.30	16.20	3.48	0.04	0.07	0.06	0.32	0.03	1.29	0.04	17.84
JM1F	73.77	11.70	3.41	0.02	0.05	0.04	0.45	0.03	1.20	0.04	7.26
JM1K	67.51	14.01	2.95	0.03	0.06	0.05	0.32	0.03	1.25	0.05	13.65
JM2A	49.75	23.80	4.90	0.04	0.32	0.05	0.94	0.03	1.74	0.12	16.68
JM2C	52.38	16.00	5.23	0.16	0.26	0.15	1.05	0.04	1.67	0.06	16.91
JM3B	65.31	11.57	5.35	0.03	0.11	0.04	0.93	0.05	1.26	0.04	15.60
JM3C	56.17	12.67	5.86	0.16	0.22	0.10	1.07	0.05	1.40	0.07	19.11
OG2A	48.55	9.55	24.51	0.40	0.16	0.04	0.55	0.05	1.43	0.55	12.25
OG2B	65.16	10.51	8.09	0.03	0.13	0.06	1.07	0.04	1.56	0.07	8.55
OG2E	49.60	23.78	2.39	0.03	0.09	0.03	0.48	0.02	1.40	0.08	19.99
OG2H	6.67	2.20	1.12	0.09	0.03	0.01	0.02	0.01	0.18	0.02	89.74
OG2L	48.59	20.60	13.17	0.06	0.18	0.04	0.62	0.26	1.49	0.09	15.7
OG2M	2.64	0.95	1.15	0.16	0.04	0.01	0.05	0.02	0.10	0.01	94.06
OG2U	79.65	8.56	1.86	0.06	0.06	0.02	0.21	0.02	1.48	0.04	6.03
Min.	2.64	0.95	1.12	0.02	0.03	0.01	0.02	0.01	0.10	0.01	6.03
Max.	79.65	23.80	24.51	0.40	0.32	0.15	1.07	0.26	1.74	0.55	94.06

Table 2. Some calculated geochemical proxies for the Patti formation shales at Agbaja Plateau.

Sample	Al_2O_3/ SiO_2	Fe_2O_3+ MgO	K_2O+ Na_2O	SiO_2/ Al_2O_3	Al_2O_3/ TiO_2	K_2O/ Al_2O_3	Fe_2O_3/ MnO	Al_2O_3/ MgO	Al_2O_3/ CaO	CIA	CIW	PIA
JM1C	0.22	5.25	0.56	4.46	8.63	0.04	128.75	142.40	712.00	96.09	99.58	92.58
JM1D	0.17	11.00	0.61	5.90	6.99	0.06	182.33	143.33	430.00	93.17	98.62	87.65
JM1E	0.18	6.06	0.74	5.44	7.71	0.06	99.17	112.18	411.33	94.13	99.52	88.71
JM1H	0.27	3.55	0.38	3.66	12.56	0.02	116.00	231.43	405.00	97.47	99.39	95.55
JM1F	0.16	3.46	0.49	6.31	9.75	0.04	113.67	234.00	585.00	95.82	99.49	92.14
JM1K	0.21	3.01	0.37	4.82	11.21	0.02	98.33	233.50	467.00	97.22	99.43	95.00
JM2A	0.48	5.22	0.99	2.09	13.68	0.04	163.33	74.38	595.00	95.85	99.62	92.07
JM2C	0.31	5.49	1.20	3.27	9.58	0.07	130.75	61.54	100.00	92.17	98.10	86.12
JM3B	0.18	5.46	0.97	5.64	9.18	0.08	107.00	105.18	385.67	92.04	99.40	84.65
JM3C	0.23	6.08	1.17	4.43	9.05	0.08	117.20	57.59	79.19	90.50	97.99	82.86
OG2A	0.20	24.67	0.59	5.08	6.68	0.06	490.20	59.69	23.88	90.61	95.60	85.39
OG2B	0.16	8.22	1.13	6.20	6.74	0.10	202.25	80.85	350.33	90.06	99.15	80.89
OG2E	0.48	2.48	0.51	2.09	16.99	0.02	119.50	264.22	792.67	97.78	99.75	95.81
OG2H	0.33	1.15	0.03	3.03	12.22	0.01	112.00	73.33	24.44	94.83	95.65	93.97
OG2L	0.42	13.35	0.66	2.36	13.83	0.03	50.65	114.44	343.33	96.62	99.52	93.71
OG2M	0.36	1.19	0.06	2.78	9.50	0.05	57.50	23.75	5.94	81.20	84.82	76.92
OG2U	0.11	1.92	0.23	9.30	5.78	0.02	93.00	142.67	142.67	96.72	99.07	94.35
PAAS	0.30	6.72	4.90	3.32	18.90	0.20	41.09	8.59	14.54	75.30	88.32	60.56
UCC	0.22	6.52	6.07	4.63	22.50	0.19	40.40	5.81	4.01	59.85	67.73	48.21

Table 3. Trace element composition of the Patti formation shales at Agbaja Plateau.

Sample	Co	Sc	Ba	Cr	Ga	Hf	Nb	Rb	Sr	Th	U	V	Zr	Cu	Mo	Ni
JM1C	13.10	11.80	174.20	274.00	19.80	38.60	60.20	20.90	29.50	28.52	10.01	65.00	1745.00	14.90	37.02	17.50
JM1D	11.10	8.30	148.70	435.00	14.40	46.00	43.60	20.00	23.90	25.05	10.19	75.00	1964.00	17.70	69.34	30.00
JM1E	10.60	8.70	244.40	114.00	17.50	21.80	42.70	24.80	34.00	17.81	6.64	59.00	866.00	9.30	9.78	9.80
JM1H	6.60	14.00	101.70	226.00	25.10	20.90	41.90	15.00	27.30	22.16	9.02	78.00	970.00	24.40	25.44	9.60
JM1F	4.90	8.10	135.90	248.00	17.30	11.90	37.10	16.00	28.10	14.12	4.69	60.00	550.00	12.20	34.12	12.60
JM1K	6.00	9.80	112.30	227.00	23.20	24.20	43.10	14.50	27.40	22.17	7.01	61.00	1079.00	15.00	28.92	12.50
JM2A	24.00	26.30	279.30	237.00	35.40	21.60	48.00	48.80	57.60	34.82	17.41	127.00	861.00	20.60	11.13	36.20
JM2C	26.90	25.40	276.90	229.00	25.80	41.00	59.90	48.40	50.50	37.52	18.96	87.00	1840.00	21.40	23.92	33.80
JM3B	15.60	8.70	255.00	321.00	18.50	33.60	31.40	29.00	37.60	21.25	8.77	60.00	1353.00	15.50	45.59	21.50
JM3C	26.30	11.20	373.80	329.00	21.80	29.80	112.20	35.40	63.10	26.46	10.89	75.00	1163.00	23.30	42.44	33.60
OG2A	12.30	21.70	230.80	156.00	20.10	79.70	35.40	21.10	67.10	49.87	23.33	176.00	3041.00	10.60	6.87	12.60
OG2B	23.60	13.50	314.20	133.00	15.20	63.90	50.30	35.60	41.40	35.01	13.00	96.00	2236.00	11.30	10.76	18.20
OG2E	17.80	18.40	235.60	137.00	35.60	21.70	45.50	18.80	44.00	29.42	7.67	92.00	804.00	21.50	6.15	15.70
OG2H	3.70	2.20	46.00	28.00	19.30	2.40	4.00	2.50	12.90	3.00	1.11	14.00	76.00	10.40	3.45	13.20
OG2L	17.60	14.80	225.40	106.00	26.90	15.40	37.00	25.70	41.70	22.98	5.89	100.00	552.00	18.60	4.16	12.80
OG2M	4.20	1.80	160.80	21.00	21.50	1.40	5.90	1.60	20.20	2.54	0.58	19.00	35.00	6.20	1.95	6.30
OG2U	8.50	7.70	86.90	136.00	13.80	51.60	42.60	6.80	29.40	29.87	8.82	49.00	1935.00	9.20	12.67	10.00
Min.	3.70	1.80	46.00	21.00	13.80	1.40	4.00	1.60	12.90	2.54	0.58	14.00	35.00	6.20	1.95	6.30
Max.	26.90	26.30	373.80	435.00	35.60	79.70	112.20	48.80	67.10	49.87	23.33	176.00	3041.00	24.40	69.34	36.20

Table 4. Trace element ratio of the Patti Formation shales at Agbaja Plateau.

Sample	Ni/Co	U/Th	Cr/V	Rb/Sr	La/Sc	Th/Sc	La/Th	Th/Co	Th/Cr	Cr/Ni	Cr/Th	V/Ni	La/Co	Th/U	V/Cr	Zr/Sc	Co/Th	V/Sc
JM1C	1.34	0.35	4.22	0.71	6.05	2.42	2.50	2.18	0.10	15.66	9.61	3.71	5.45	2.85	0.24	147.88	0.46	5.51
JM1D	2.70	0.41	5.80	0.84	7.27	3.02	2.41	2.26	0.06	14.50	17.37	2.50	5.43	2.46	0.17	236.63	0.44	9.04
JM1E	0.92	0.37	1.93	0.73	5.30	2.05	2.59	1.68	0.16	11.63	6.40	6.02	4.35	2.68	0.52	99.54	0.60	6.78
JM1H	1.45	0.41	2.90	0.55	4.92	1.58	3.11	3.36	0.10	23.54	10.20	8.13	10.44	2.46	0.35	69.29	0.30	5.57
JM1F	2.57	0.33	4.13	0.57	4.43	1.74	2.54	2.88	0.06	19.68	17.56	4.76	7.33	3.01	0.24	67.90	0.35	7.41
JM1K	2.08	0.32	3.72	0.53	5.94	2.26	2.63	3.70	0.10	18.16	10.24	4.88	9.70	3.16	0.27	110.10	0.27	6.22
JM2A	1.51	0.50	1.87	0.85	5.14	1.32	3.88	1.45	0.15	6.55	6.81	3.51	5.63	2.00	0.54	32.74	0.69	4.83
JM2C	1.26	0.51	2.63	0.96	3.55	1.48	2.40	1.39	0.16	6.78	6.10	2.57	3.35	1.98	0.38	72.44	0.72	3.43
JM3B	1.38	0.41	5.35	0.77	6.38	2.44	2.61	1.36	0.07	14.93	15.11	2.79	3.56	2.42	0.19	155.52	0.73	6.90
JM3C	1.28	0.41	4.39	0.56	5.63	2.36	2.38	1.01	0.08	9.79	12.43	2.23	2.40	2.43	0.23	103.84	0.99	6.70
OG2A	1.02	0.47	0.89	0.31	15.21	2.30	6.62	4.05	0.32	12.38	3.13	13.97	26.84	2.14	1.13	140.14	0.25	8.11
OG2B	0.77	0.37	1.39	0.86	5.27	2.59	2.03	1.48	0.26	7.31	3.80	5.27	3.01	2.69	0.72	165.63	0.67	7.11
OG2E	0.88	0.26	1.49	0.43	4.89	1.60	3.06	1.65	0.21	8.73	4.66	5.86	5.06	3.84	0.67	43.70	0.61	5.00
OG2H	3.57	0.37	2.00	0.19	3.91	1.36	2.87	0.81	0.11	2.12	9.33	1.06	2.32	2.70	0.50	34.55	1.23	6.36
OG2L	0.73	0.26	1.06	0.62	4.24	1.55	2.73	1.31	0.22	8.28	4.61	7.81	3.56	3.90	0.94	37.30	0.77	6.76
OG2M	1.50	0.23	1.11	0.08	3.44	1.41	2.44	0.60	0.12	3.33	8.27	3.02	1.48	4.38	0.90	19.44	1.65	10.56
OG2U	1.18	0.30	2.78	0.23	8.97	3.88	2.31	3.51	0.22	13.60	4.55	4.90	8.13	3.39	0.36	251.30	0.28	6.36

7

Table 5. Rare Earth Element (REE) concentrations of the Patti Formation shales at Agbaja Plateau.

Sample	La	Ce	Pr	Nd	Sm	Eu	Gd	Tb	Dy	Ho	Er	Tm	Yb	Lu	Total REE
JM1C	71.40	142.80	16.27	60.00	11.14	1.58	10.63	1.70	11.64	2.54	7.75	1.19	8.31	1.27	348.22
JM1D	60.30	125.50	13.34	53.60	10.02	1.38	9.75	1.64	11.00	2.46	7.78	1.20	8.40	1.35	307.72
JM1E	46.10	99.20	10.53	42.70	7.81	1.56	7.28	1.21	7.79	1.67	5.25	0.79	5.39	0.86	238.14
JM1H	68.90	157.30	18.06	68.20	12.60	2.18	12.14	1.83	11.09	2.26	6.97	1.03	6.61	1.01	370.18
JM1F	35.90	70.40	8.21	29.10	5.43	0.95	4.49	0.73	4.54	0.98	2.88	0.44	2.85	0.47	167.37
JM1K	58.20	116.80	13.44	49.00	9.12	1.44	8.37	1.30	8.18	1.68	5.12	0.78	5.14	0.77	279.34
JM2A	135.10	290.10	28.17	115.00	19.99	4.25	17.55	2.55	15.04	3.00	8.72	1.27	8.45	1.29	650.48
JM2C	90.10	188.70	21.04	77.80	14.50	2.28	13.30	2.19	14.66	3.16	9.85	1.53	10.16	1.58	450.85
JM3B	55.50	114.20	12.28	49.80	9.23	1.66	8.89	1.47	9.42	2.06	6.31	0.95	6.52	1.04	279.33
JM3C	63.00	130.50	14.26	57.70	10.79	2.04	9.72	1.55	10.00	2.14	6.66	0.97	6.55	1.05	316.93
OG2A	330.10	726.20	70.18	290.20	49.27	9.60	39.36	5.86	37.02	7.53	14.89	2.84	21.46	2.86	1607.37
OG2B	71.10	154.80	16.51	64.70	12.54	2.07	10.08	1.94	14.51	3.25	9.99	1.48	11.66	1.40	376.03
OG2E	90.00	176.10	18.74	72.30	13.11	2.26	10.28	1.63	11.37	2.10	7.36	0.86	6.79	0.79	413.69
OG2H	8.60	19.50	2.26	8.80	1.79	0.34	1.55	0.24	1.42	0.30	0.98	0.12	0.73	0.13	46.76
OG2L	62.70	131.10	14.00	54.60	10.53	1.85	8.01	1.24	8.33	1.42	5.29	0.66	4.98	0.66	305.37
OG2M	6.20	18.00	1.77	7.80	1.64	0.24	0.74	0.26	1.15	0.32	0.63	0.04	0.55	0.06	39.40
OG2U	69.10	145.90	14.96	60.70	9.99	1.31	9.61	1.56	10.43	2.35	7.48	1.01	8.01	1.12	343.53
Min.	6.20	18.00	1.77	7.80	1.64	0.24	0.74	0.24	1.15	0.30	0.63	0.04	0.55	0.06	39.40
Max.	330.10	726.20	70.18	290.20	49.27	9.60	39.36	5.86	37.02	7.53	14.89	2.84	21.46	2.86	1607.37

8

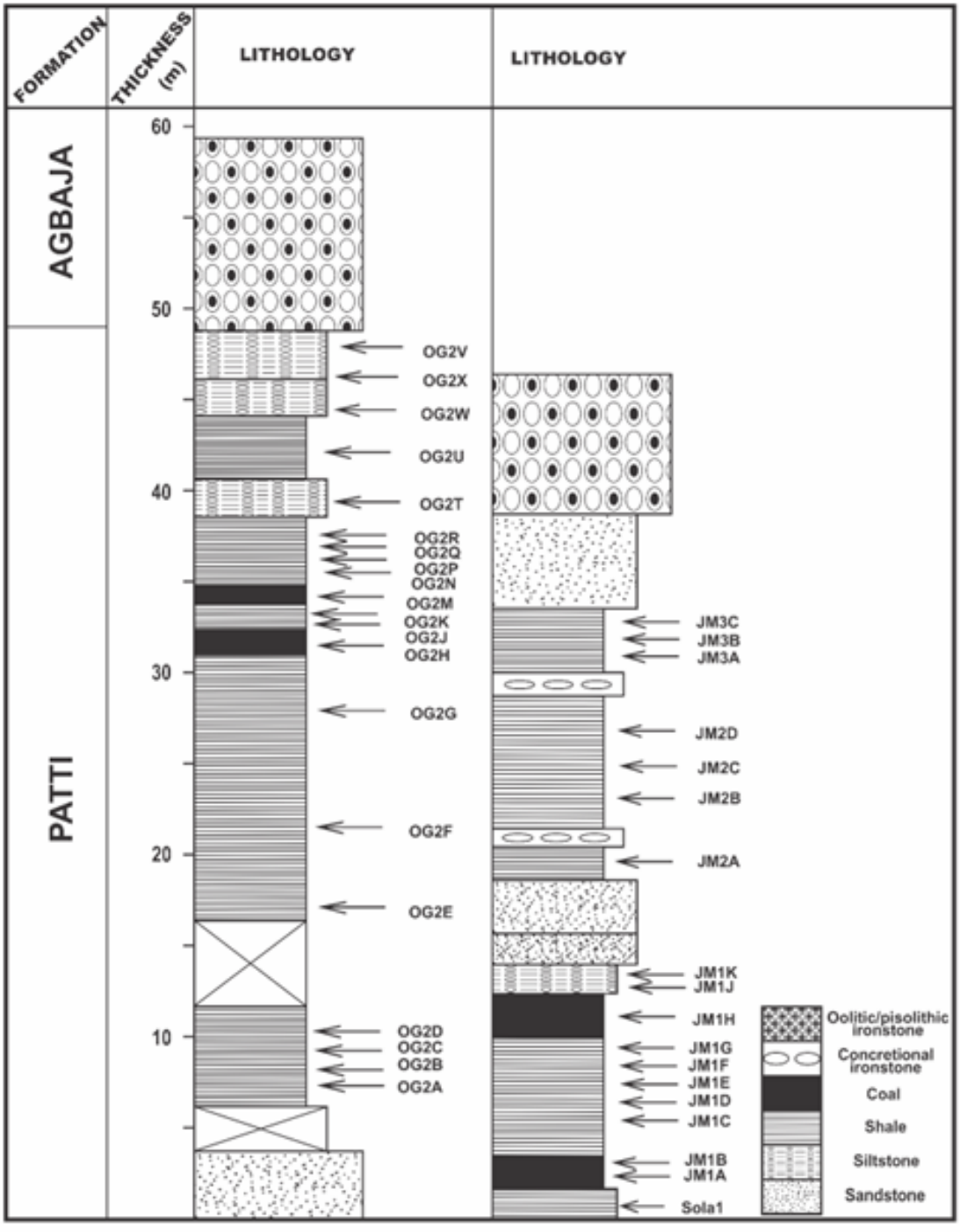

Figure 3. Vertical lithologic profiles of the investigated Patti Formation exposed at Agbaja Plateau, southern Bida Basin, Nigeria.

and Roser *et al*. [39], the values less than 3.00 (mafic), 3.00-5.00 (felsic), while values greater than 5.00 indicate progressive maturity. In the present study, SiO_2/Al_2O_3 ranges from 2.09 to 9.30% (Mean-4.52) indicating an intermediate to felsic rocks and progressive maturity. Index of Compositional Variability (ICV) proposed by Cox *et al*. [40] and calculated using the formula; $(Fe_2O_3+K_2O+Na_2O+CaO+MgO+MnO+TiO_2)/Al_2O_3$ was also employed in this study. According to the authors, ICV values greater than 1.00 (>1) indicate more rock-forming minerals, whereas, rocks with lesser clay minerals will show ICV values less than 1.00 (<1). In this study, the relatively high ICV values of the studied shales range from 0.19 to 284 with a mean of 0.80 suggests progressive compositional maturity. Figure 4a after Crook [41] displays the Na2O–K2O bivariate classification plot, which shows that the shales are high in quartz, and Figure 4b after McLennan *et al*. [13] displays their relatively

Table 6. REE calculated ratios, anomalies, and normalized values of the Patti Formation shales at Agbaja Plateau.

Sample	∑LREE	∑HREE	∑LREE/∑HREE	Eu/Eu*	Ce/Ce*	$(La/Lu)_N$	$(La/Yb)_N$	$(Gd/Yb)_N$
JM1C	301.61	45.03	6.70	0.44	0.95	5.84	5.79	1.03
JM1D	262.76	43.58	6.03	0.43	0.97	4.64	4.84	0.94
JM1E	206.34	30.24	6.82	0.63	1.00	5.57	5.77	1.09
JM1H	325.06	42.94	7.57	0.54	1.05	7.09	7.03	1.48
JM1F	149.04	17.38	8.58	0.59	0.93	7.93	8.49	1.27
JM1K	246.56	31.34	7.87	0.50	0.95	7.85	7.63	1.31
JM2A	588.36	57.87	10.17	0.69	1.01	10.88	10.78	1.68
JM2C	392.14	56.43	6.95	0.50	0.99	5.92	5.98	1.06
JM3B	241.01	36.66	6.57	0.56	0.96	5.54	5.74	1.10
JM3C	276.25	38.64	7.15	0.61	0.96	6.23	6.48	1.20
OG2A	1465.95	131.82	11.12	0.67	1.03	11.99	10.37	1.48
OG2B	319.65	54.31	5.89	0.56	1.01	5.27	4.11	0.70
OG2E	370.25	41.18	8.99	0.60	0.93	11.84	8.94	1.22
OG2H	40.95	5.47	7.49	0.62	1.03	6.87	7.95	1.71
OG2L	272.93	30.59	8.92	0.62	0.98	9.87	8.49	1.30
OG2M	35.41	3.75	9.44	0.67	1.26	10.75	7.60	1.09
OG2U	300.65	41.57	7.23	0.41	0.99	6.41	5.82	0.97
Min.	35.41	3.75	5.89	0.41	0.93	4.64	4.11	0.70
Max.	1465.95	131.82	11.12	0.69	1.26	11.99	10.78	1.71

high compositional maturity based on Zr/Sc and Th/Sc ratios.

Chemical weathering and maturity trend of sediments from the source area can also be assessed using various geochemical proxies including; CIA calculated as $[Al_2O_3/(Al_2O_3+CaO+Na_2O+K_2O)]\times100$ after Nesbitt and Young [42], CIW calculated as $[Al_2O_3/(Al_2O_3+CaO+Na_2O)]\times100$ after Harnois [43] and PIA calculated as: $[(Al_2O_3-K_2O)/(Al_2O_3+CaO+Na_2O-K_2O)]\times100$ after Fedo *et al.* [44]. According to Fedo *et al.* [45] and Descourvieres *et al.* [46], CIA values between 50.0 and 60.0 indicate low chemical weathering degree, whereas, values between 60.0 and 80.0 indicate moderate weathering, while values greater than 80.0 indicate intense chemical weathering. Similarly, Depetris and Probst [47] proposed CIW values less than 50 for chemically un-weathered source rock, values ranging between 51 and 75 for moderate weathering and values greater than 75 is an indication of strong weathering in the source area. The high CIA (81.20–97.78), CIW (84.82–99.75), and PIA (76.92–95.81) values indicate strong chemical weathering in the source area. This is probably because the rocks have been exposed to weathering agents for a long time in humid conditions in the source area.

In an effort to further determine the degree of chemical weathering of the studied shale samples, bivariate plots of SiO_2 versus $(Al_2O_3+Na_2O+K_2O)$ after Suttner and Dutta [9], SiO_2 (%) versus CIA after [42], and Al_2O_3 (%) versus CIA after Ref. [48] were constructed, and the diagrams reveal sample clustering within intense weathering zone (Figures 4c, 4d, & 4e) which confirm increasing chemical weathering and maturity trend for the investigated shales. Ternary diagrams of A-CN-K $\{Al_2O_3–(CaO+Na_2O)–K_2O\}$ after Ref. [49] and A-CNK-FM $(Al_2O_3–CaO^*+Na_2O+K_2O–Fe_2O_3+MgO)$ after [50] also indicating high weathering intensity for the studied shales (Figure 4f and 4g). Therefore, the results show that the Patti Formation's depositional characteristics align with a source area that experienced intense weathering in tropical to subtropical climates.

5.2. Provenance

The provenance history of the silica rich sediments, according to Bhatia and Crook [8], can be revealed from their detrital framework grain composition. Garcia *et al.* [51] opined that Al_2O_3/TiO_2 ratios are useful for clastic source rock composition identification. Certain range of values were suggested as provenance discriminants; 3.00–8.00 for mafic sourced igneous rocks, 8.00–21.00 for an intermediate sourced igneous rock, while 21.00–70.00 for felsic sourced igneous rocks. The values of Al_2O_3/TiO_2 for the shales from Agbaja range from 5.78-16.99 (Mean 10.00) indicating an intermediate source rock (Table 2). The values of the studied samples also compare relatively well with the standard published values (PAAS - 18.90, and UCC - 22.50), therefore indicating similar source rock signature. Meanwhile, the elements-based provenance discriminant bivariate plots of SiO_2 (%) versus Al_2O_3/TiO_2 after Le Bas *et al.* [52], Zr versus TiO_2 and Ni versus TiO_2 after Hayashi *et al.* [53], indicate that the shales were derived from the felsic igneous rocks (Figures 5a, 5b, and 5c).

The contrasting behavior and characteristics of some trace elements (e.g. Ba, Rb, Th, Sc, Co, Cr, Nb and La) in clastic sediments are helpful provenance indicators [13]. Condie and Wronkicwiez [54] stated that immobile trace elements including Sc, Co and Cr with lower concentration of the mobile trace elements like La and Th are significantly higher in concentration within basic source rocks whereas felsic source rocks comprise of lower immobile trace elements concentration

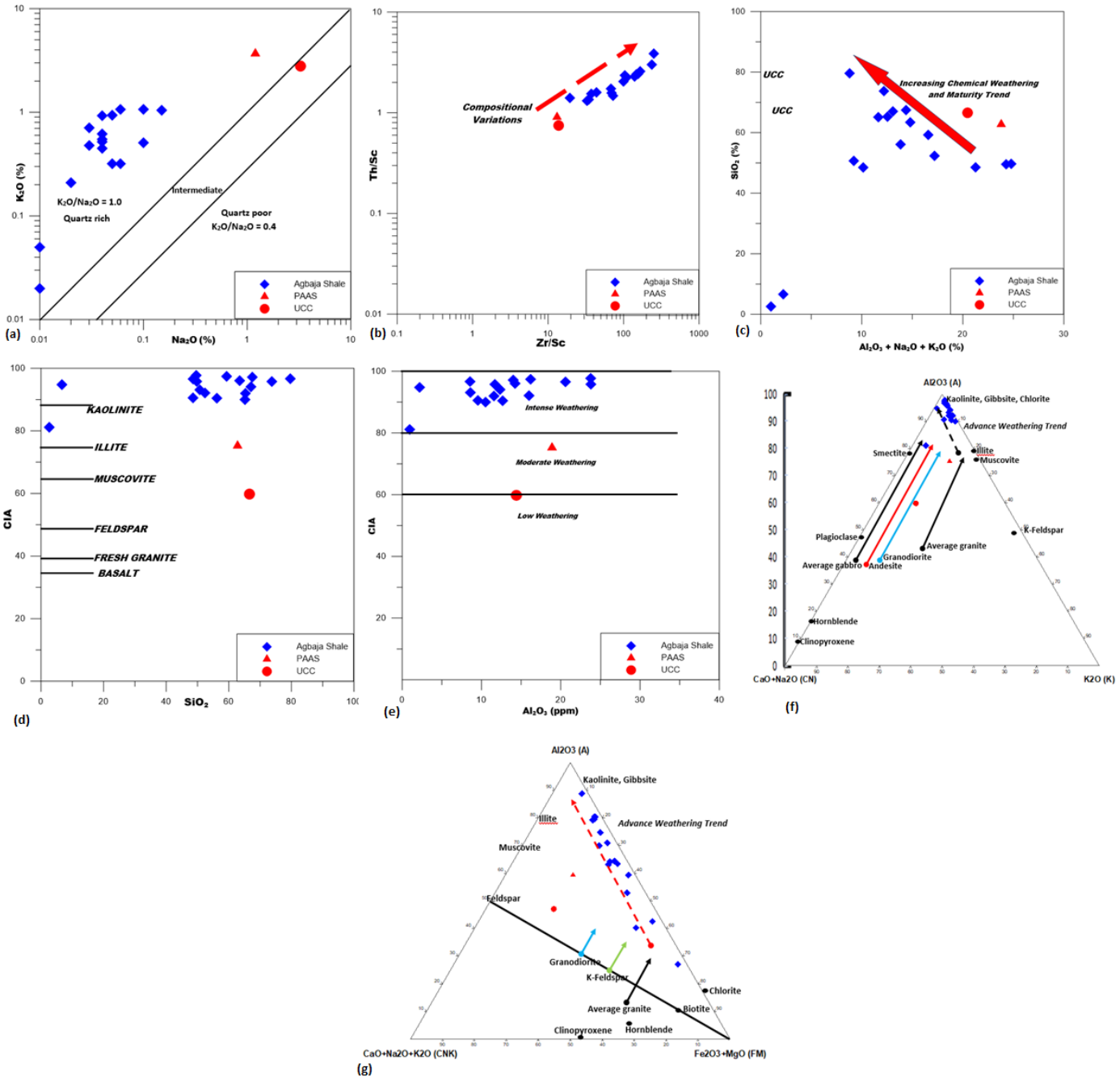

Figure 4. (a) Bivariate classification plot Na_2O (%) versus K_2O (%) after Crook [41] showing quartz rich sediments (b) Bivariate compositional maturity plot of Th/Sc versus Zr/Sc after McLennan *et al.* [13] indicating higher compositional maturity (c) Bivariate paleoweathering plot of Al_2O_3+K_2O+Na_2O (%) versus SiO_2 (%) after [9] showing increasing in the chemical weathering and maturity trend (d) Bivariate paleoweathering plot of SiO_2 versus CIA after [42] showing the weathering trends and likely mineralogical composition in the studied samples (e) Bivariate paleoweathering plot of AlO_2O_3 versus CIA after [48] indicating intense weathering conditions during deposition of the Patti Shale. (f) Ternary paloweathering plot of A-CN-K {Al_2O_3-(Na_2O+CaO)-K_2O} after [49] showing advance weathering trends of the investigated shale compared with some typical source rocks (g) Ternary paleoweathering plot of A-CNK-FM {Al_2O_3-(Na_2O+CaO+K_2O)-(Fe_2O_3+MgO)} after [50] showing advance weathering trends of the investigated shale compared with some typical source rocks.

with higher concentrations of mobile trace elements. Taylor and Mclennan [7], Cullers [55, 56], Condie and Wronkiewicz [57] and many others have also employed trace element ratios (e.g. La/Th, La/Co, Th/Co, La/Sc, Th/Sc, Cr/Th, Th/Co, Ba/Rb, Zr/Nb, Zr/Hf and Zr/Th) and considered them to be sensitive to variations in the basic and silicic source rocks provenance. Basu *et al.* [58] opined that differences between felsic and mafic sources can be ascertained using the ratios such as La/Co, La/Sc, Th/Sc and Th/Co. Most calculated trace element ratios for the studied shales (Tables 3 and 4) conform with the

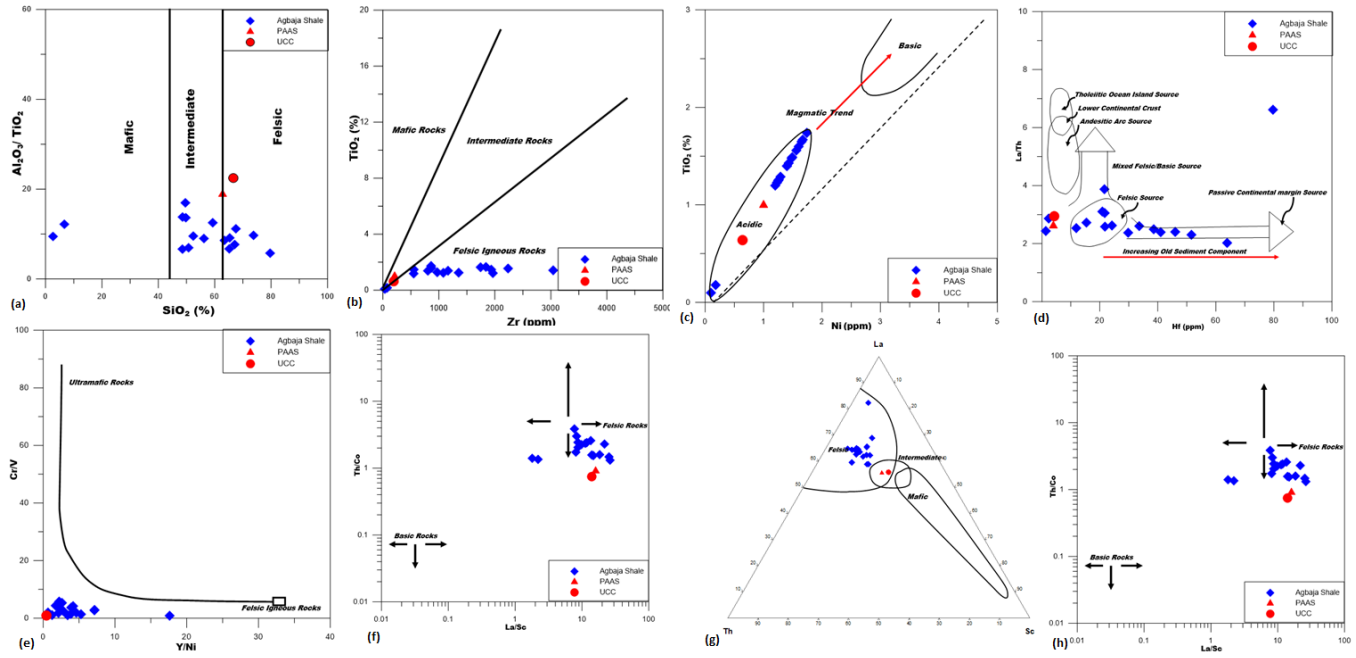

Figure 5. (a) Bivariate provenance discrimination plot SiO_2 versus Al_2O_3/TiO_2 after [52] showing dominance of intermediate to felsic source rocks. (b) Bivariate provenance discrimination plot Zr (ppm) versus TiO_2 after [53] showing sediments derivation from felsic igneous rocks. (c) Bivariate provenance discrimination plot of Ni (ppm) versus TiO_2 after [53] indicating acidic source rocks (d) Bivariate provenance discrimination plot Hf (ppm) versus La/Th after [61] indicating felsic source rocks (e) Bivariate provenance discrimination plot Y/Ni versus Cr/V after [61] indicating felsic igneous rocks derivation (f) Bivariate provenance discrimination plot of Th/Co versus La/Sc after [62] indicating felsic igneous rocks derivation (g) Ternary provenance discrimination plot of La-Th-Sc after [62] showing felsic field for the investigated sandstones (h) Ternary provenance discrimination plot of V-Ni-Th*10 after [63] showing felsic fields.

published data, and this therefore support the inference of sediments derivation from felsic source rocks. Several discriminant plots; e.g. bivariate (Figures 5d, 5e, and 5f) and ternary (Figures 5g and 5h) also show samples clustering within felsic rock source field.

Rare earth elements data were also employed in this work to corroborate the major oxide and trace elements in the determination of the provenance of the shales. According to Bhatia, M.R., and Crook [8], Cullers [55], Condie and Wronkiewicz [57], and McLennan *et al.* [59], felsic rocks are usually enriched in LREE and LREE/HREE ratios, whereas mafic rocks normally exhibit low LREE and LREE/HREE ratio. Taylor and Mclennan [7], McLennan *et al.* [13], and Cullers and Graft [60] had suggested that europium anomaly (Eu/Eu*) in the sedimentary rocks provide clues for the source rock characteristics because felsic rocks are characterized by negative Eu/Eu* (<1.0) whereas the mafic rocks exhibit positive but low Eu/Eu* (>1.0). All the samples show pronounced negative Eu anomalies, which indicated granitic source, whereas, values of Ce anomalies reflect an oxidizing to weak reducing environment. Tables 5 and 6 indicate high ∑REE, LREE enrichment than HREE, high LREE/HREE ratios and negative Eu/Eu* in the shale samples from Agbaja which corroborate other proxies of felsic protolith. The calculated values of some REE geochemical proxies in this study are also consistent with the published data of PAAS and UCC which also support felsic source rocks origin with a suggestion that the sediments could have been eroded from the adjacent granitic crystalline basement. The mean values of normalized La/Yb $(La/Yb)_N$, and Gd/Yb $(Gd/Yb)_N$ are also in support of felsic source rocks in the southern Bida Basin.

5.3. *Tectonic setting*

The tectonic setting is an important aspect of the basin analytical studies as it controls the geological structures, sedimentation styles and mineral resources. Good number of authors including Bhatia [4], Bhatia and Crook [8], Roser and Korsch [38], Maynard *et al.* [64], and Roser and Korsch [65] have used sediment composition to infer the tectonic settings of sedimentary rocks. For example, Floyd and Leveridge [61] and McLennan and Taylor [67] have employed major and trace element compositions to determine the tectonic settings of sedimentary rocks. They opined that concentrations of SiO_2 and ratio of K_2O/Na_2O of sedimentary rocks are sensitive indicators of paleotectonic settings, for instance, the magmatic island arcs are characterized by quartz-poor greywackes with 58% SiO_2 and K_2O/Na_2O of <1.00 while Andean-type continental margins quartz with intermediate greywackes are composed of 68-74% SiO_2 and <1.00 K_2O/Na_2O and this is also indicative of upper continental crust, whereas, sediments in Atlantic-type continental margins are characterized by quartz-rich greywackes with 89% SiO_2 and >1.00 K_2O/Na_2O. The mean value of SiO_2 and

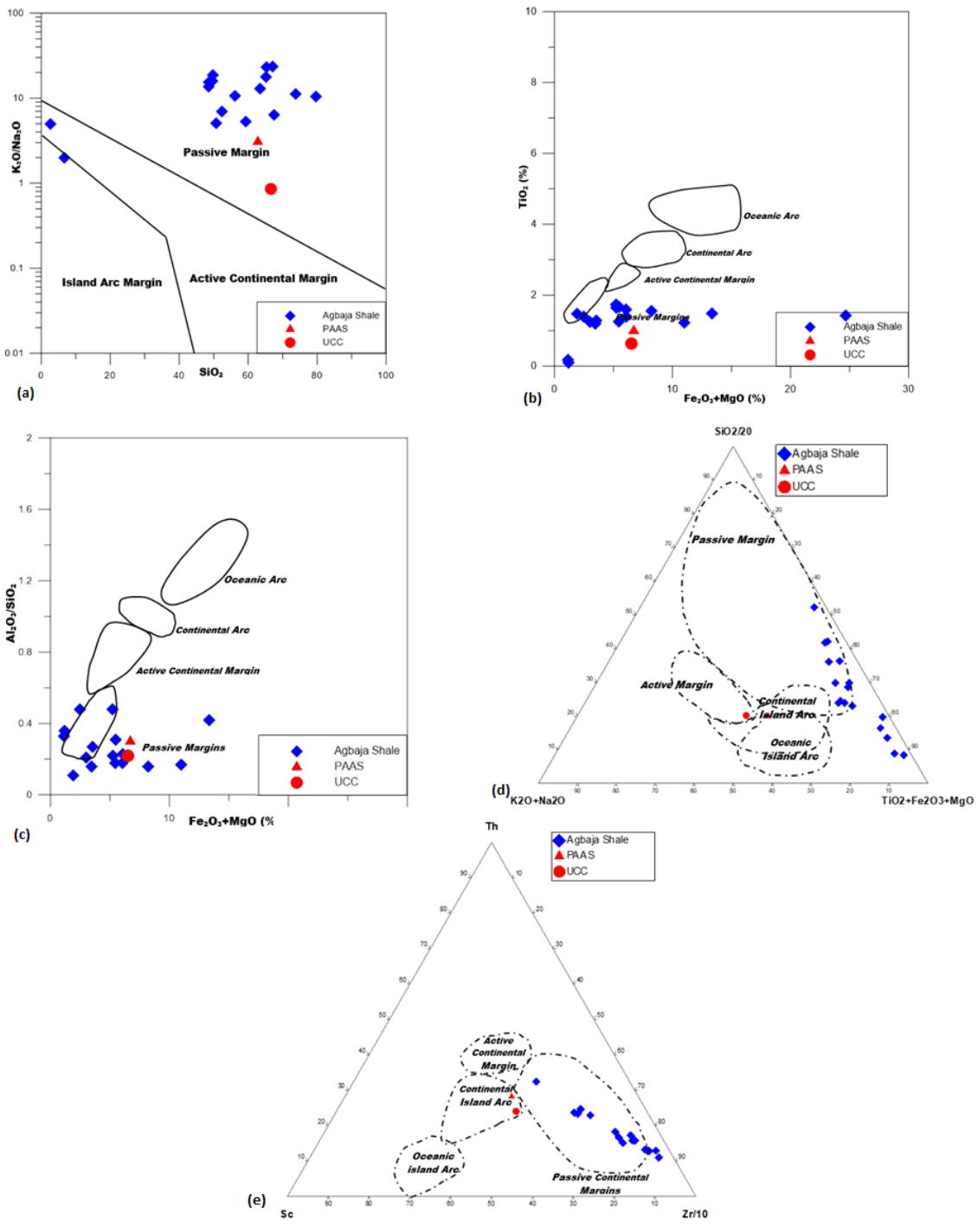

Figure 6. (a) Bivariate paleotectonic plot of SiO_2 versus K_2O/Na_2O after [38] indication Passive Margin settings (b) Bivariate Paleotectonic plot of Fe_2O_3+MgO versus TiO_2 after [4] (c) Bivariate Paleotectonic plot of Fe_2O_3+MgO versus Al_2O/SiO_2 after [4] (d) Ternary paleotectonic plot of $SiO_2/20$-(K_2O+Na_2O)-(TiO_2+Fe_2O_3+MgO) after [14]. Note, the investigated shales fall within the passive margin field (e) Ternary paleotectonic plot of Th-Sc-Zr/10 after [4]. Note that the investigated shales fall within the passive margin field.

K_2O/Na_2O in this study (Table 1 and 2) relatively fits into passive paleotectonic setting. Trace elements compositions and the ratios are also very useful for past tectonic settings reconstruction in sedimentary rocks [8]. According to Bhatia and Crook [8], low content of Sc with high Zr/Th ratio in sandstones are typical of a recycled passive tectonic margin setting. In this study, the values of Sc and Zr/Th (Tables 5 and 6) conform with the characteristics of sediments of the passive margin paleotectonic settings. Similarity of rare earth element (REE) values in this study with the PAAS and UCC also indicate passive continental margin tectonic settings (Tables 5 and 6).

Various paleotectonic discrimination plots; including

$\log(K_2O/Na_2O)$ versus SiO_2(%) after [38], TiO_2(%) versus Fe_2O_3+MgO(%) after [4], Al_2O_3/SiO_2 versus Fe_2O_3+MgO(%) after [4], and SiO_2/20-K_2O+Na_2O(%)-TiO_2+Fe_2O_3+MgO(%) after [14] have been employed in previous studies for paleotectonic settings determination (e.g. passive continental margin-PM, active continental margin-ACM, continental island arc-CIA, and oceanic island arc-OIA) of sedimentary rocks and these are adopted in this present work. Based on the discriminant diagrams presented in Figures 6a, 7b, and 7c, the Agbaja shales were sourced from the passive margin paleotectonic settings. Also, the discriminant ternary plots of SiO_2/20-(K_2O+Na_2O)-(TiO_2+Fe_2O_3+MgO) after [14], La-Th-Sc and Th-Sc-Zr/10 after [8] also substantiate the inferred passive continental margin tectonic setting for the investigated shales (Figure 6d, and 6e).

6. Regional correlation with some other rifted basins

gross geochemical characteristics of the shales from the Bida basin (major trace, and rare earth elements) reflect a passive margin basin which are typically formed after tectonic rifting and are characterized by long-term subsidence. Generally, the following characteristics which have been documented in some passive margin related sedimentary basins in Africa are; lower levels trace elements like Cr, Ni, and Fe like which suggests more stable margin like in Anambra basin and Iullemmeden, quartz-rich sediments and the presence of aluminosilicates (Al_2O_3) which reflects a stable cratonic provenance, dominated by weathering of older continental rocks like in Tano basin, Ghana. Relatively high Zr and Ti enrichment: zirconium (Zr) and titanium (Ti) which are probably due to the concentration of heavy minerals like zircon and rutile, which are resistant to weathering suggesting accumulation of mature sediments after prolonged transport and sorting process. Other features of the investigated shales are enrichment of Light REEs (LREEs) in light rare earth elements (LREEs) compared to heavy rare earth elements (HREEs) and negative europium (Eu) anomaly. This pattern also suggests felsic source provenance. The shales from Agbaja are typically rich in silicates (SiO_2) from quartz and aluminosilicate minerals (Al_2O_3), reflecting a felsic continental crustal source. It is interesting to note that the above characteristics obtained from the Bida Basin show compelling similarities with the very well know passive margin basins **N**iger Delta (Nigeria) [68], the Amazon Fan (South America) [69] and Tano basin [13]. Zobah *et al*. [70] reported that the shallow marine sourced sediments from Voltaian Basin, Ghana have a felsic source with some inputs from metasedimentary rocks within a semi-humid climate condition. The sediments were suggested to have been derived from recycled sedimentary rocks in a passive continental margin with possible sediments from the Pan African Orogeny. Within the context of gross geochemistry and the thick sequences of continental to marine shales and sandstones, there is little tectonic activity, typically after rifting processes have ceased and a stable phase would have been attained in the Bida Basin suggesting passive margin and high weathering.

7. Conclusions

The present study employed bulk inorganic geochemical compositions to reconstruct the paleotectonic and provenance history of the studied lithologies from the Patti Formation exposed at the Agbaja Plateau, in the southern Bida Basin, Central Nigeria. The study suggests that the shale samples were predominantly derived from the adjacent Pan African reactivated felsic igneous rocks.

The elemental proxies such as relatively high Al_2O_3, CIA, CIW and PIA values, with low Na_2O/Al_2O_3, Na_2O/K_2O and Na_2O/TiO_2 ratios as well as other discrimination plots indicated that the sediments had undergone intense chemical weathering at the source areas and they are highly mature compositionally.

Several paleotectonic proxies applied (e.g. The La-Th-Sc diagram) indicates that the sediments originate from a passive margin tectonic setting, with the negative Eu anomaly pointing to the felsic composition of the source rocks. The tectonic history of the Bida Basin therefore compares closely with other rift basins from West Africa like Tano, Voltaian Ghana.

Overall, the geochemical data indicates that the shales are compositionally mature, sourced from an area subjected to intensive chemical weathering. This suggests a stable tectonic environment and significant sediment recycling.

Data availability

We do not have any research data outside the submitted manuscript file.

Acknowledgement

The first author thanked the Government of Federal Republic of Nigeria for the Tetfund National Research Fund (NRF) Grant Intervention and the management of the Federal University of Oye-Ekiti for providing the institutional support for the conduct the research.

References

[1] A.J. Edegbai, L. Schwark, & F. E. Oboh-Ikuenobe, "Nature of dispersed organic matter and paleoxygenation of the Campano-Maastrichtian dark mudstone unit, Benin flank, western Anambra Basin: Implications for Maastrichtian Trans-Saharan seaway paleoceanographic conditions", Journal of African Earth Sciences **162** (2019) 103654. https://doi.org/10.1016/j.jafrearsci.2019.103654.

[2] W. R. Dickinson & C. A. Suczek, "Plate tectonics and sandstone compositions", American Association of Petroleum Geologists Bulletin **63** (1979) 2182. https://doi.org/10.1306/2F9188FB-16CE-11D7-8645000102C1865D

[3] M. R. Bhatia, "1985. Rare earth element geochemistry of Australian Paleozoic graywackes and mudrocks: Provenance and tectonic control", Sedimentary Geology **45** (1985) 113. https://doi.org/10.1016/0037-0738(85)90025-9.

[4] M. R. Bhatia, 1983, "Plate tectonics and geochemical composition of sandstones", The Journal of Geology **91** (1983) 627. https://doi.org/10.1086/628815.

[5] W. R. Dickinson, L. S. Beard, G. R. Brakenridge, J. L. Evjavec, R. C. Ferguson, K. F. Inman, R. A. Knepp, F. A. Lindberg, & P. T. Ryberg, "Provenance of North American Phanerozoic sandstones in relation to tectonic setting", Geological Society of America Bulletin **94** 1982 234. https://ui.adsabs.harvard.edu/link_gateway/1983GSAB...94..222D/doi:10.1130/0016-7606(1983)94%3C222:PONAPS%3E2.0.CO;2.

[6] H. Dypvik, "Geochemical Compositions and Depositional Conditions of Upper Jurassic and Lower Cretaceous Yorkshire Clays, England", Geological Magazine **121** (1984) 504. https://doi.org/10.1017/S0016756800030028.

[7] S. R. Taylor & S. M. Mclennan, "An examination of the geochemical record preserved in sedimentary rocks", *The Continental Crust: Its Composition and Evolution*, Blackwell Scientific Publications, U.K, Oxford, 1985, pp. 300–312. https://www.scirp.org/reference/referencespapers?referenceid=1868332.

[8] M. R. Bhatia & K. A. W. Crook "Trace element characteristics of graywackes and tectonic setting discrimination of sedimentary basins", Contributions to Mineralogy and Petrology **92** (1986) 193. https://doi.org/10.1007/BF00375292.

[9] L. J. Suttner & P. K. Dutta, "Alluvial sandstone deposition and paleoclimate, I. Framework mineralogy" Journal of Sedimentary Petrology **56** (1986) 344. https://doi.org/10.1306/212F8909-2B24-11D7-8648000102C1865D.

[10] F. J. Pettijohn, P. E. Potter & R. Siever, *Sand and Sandstone*, Springer, Berlin, 1987, pp. 523–553. http://dx.doi.org/10.1007/978-1-4612-1066-5.

[11] S. M. Mclennan, "Rare earth elements in sedimentary rocks; influence of provenance and sedimentary processes", in *Geochemistry and Mineralogy of Rare Earth Elements*, B. R. Lipin, & G. A. McKay (Eds.), Reviews in Mineralogy, Houston, Texas, USA, 1989, pp. 192–200. https://doi.org/10.1515/9781501509032-010.

[12] G. Dera, P. Pellenard, P. Neige, J. Deconinck, E. Pucéat & J. L. Dommergues, "Distribution of clay minerals in Early Jurassic Peritethyan seas: palaeoclimatic significance inferred from multiproxy comparisons", Palaeogeography, Palaeoclimatology, Palaeoecology **271** (2009) 51. https://doi.org/10.1016/j.palaeo.2008.09.010.

[13] S. M. Mclennan, S. Hemming, D. K. Mcdaniel & G. N. Hanson, "Geochemical approaches to sedimentation, provenance and tectonics", in *Processes Controlling the Composition of Clastic Sediments*, M. J. Johnsson & A. Basu (Eds.), Special Paper of Geological Society of America, USA, 1993, pp. 40–284. https://doi.org/10.1130/SPE284-p21.

[14] S. B. Kroonenberg, *Effects of Provenance, sorting and weathering on the geochemistry of fluvial sands from different tectonic and climatic environment*, Proceedings of the 29th International Geological Congress, Part A, 1994, pp. 69–81. https://www.researchgate.net/publication/40207477.

[15] G. J. Weltje, X. D. Meijer & P. L. de Boer, "Stratigraphic inversion of siliciclastic basin fills: a note on the distinction between supply signals resulting from tectonic and climatic forcing", Basin Research **10** (1998) 153. https://doi.org/10.1046/j.1365-2117.1998.00057.x.

[16] J. S. Armstrong-Altrin, Y. I. Lee, S. P. Verma & S. Ramasamy, "Geochemistry of sandstones from the upper Miocene Kudankulam Formation, southern India: Implications for provenance, weathering, and tectonic setting", Journal of Sedimentary Research **74** (2004) 297. https://doi.org/10.1306/082803740285.

[17] J. S. Armstrong-Altrin, & S. P. Verma, "Critical evaluation of six tectonic setting discrimination diagrams using geochemical data of Neogene sediments from known tectonic settings", Sedimentary Geology **177** (2005) 129. https://doi.org/10.1016/j.sedgeo.2005.02.004.

[18] O. J. Ojo, S. A. Adepoju & D.A. Adedoyin "Combined Petrographic and Geochemical Studies of Maastrichtian Patti Formation Sandstone, Bida Basin, Nigeria: Implications for Provenance and Compositional Maturity", Ilorin Journal of Science **2** (2015) 189. https://iljs.org.ng/index.php/iljs/article/view/85.

[19] M. E. Nton & O. J. Adamolekun, "Sedimentological and geochemical characteristics of outcrop sediments of southern Bida Basin, Central Nigeria: Implications for provenance, paleoenvironment and tectonic history" Ife Journal of Science **18** (2016) 369. https://www.ajol.info/index.php/ijs/article/view/144823.

[20] S. I. Bankole, A. Akinmosin, T. Omeru & H. E. Ibrahim, "Heavy Mineral Distribution in the Lokoja and Patti Formations, Southern Bida Basin, Nigeria: Implications for Provenance, Maturity and Transport History" RMZ – Materials and Geoenvironment **66** (2019) 198. https://doi.org/10.2478/rmzmag-2019-0011.

[21] O. J. Ojo, S. A. Adepoju A. Awe & M. O. Adeoye, "Mineralogy and geochemistry of the sandstone facies of Campanian Lokoja Formation in the Southern Bida basin, Nigeria: implications for provenance and weathering history" Heliyon **7** (2021) e08564. https://doi.org/10.1016/j.heliyon.2021.e08564.

[22] L. C. King, "Outline and distribution of Gondwanaland" Geological Magazine **87** (1950) 359. http://dx.doi.org/10.1017/S0016756800077311.

[23] W. Q. Kennedy, "The influence of basement structure on the evolution of the coastal (Mesozoic and Tertiary) basins", Proceedings of the Institute of Petroleum Geologists Society, London on Recent Basins around Africa, 1965, pp. 35–47. http://dx.doi.org/10.1144/jgs.157.6.1179.

[24] D. R. Adeleye, "Origin of Ironstones, an example from the Middle Niger Basin, Nigeria", Journal of Sedimentary Petrology **43** (1972) 727. https://doi.org/10.1306/74D7284C-2B21-11D7-8648000102C1865D.

[25] S. B. Ojo, & D. E. Ajakaiye, "Preliminary interpretation of gravity measurements in the middle Nıger Basin area, Nigeria" in Geology of Nigeria, 2nd ed. C.A. Kogbe (Ed.), Elizabethan Publishing Company, Lagos, 1989, pp. 347–358. https://www.scirp.org/reference/referencespapers?referenceid=1791025.

[26] C. A. Kogbe, D. E. Ajakaiye & G. Matheis, "Confirmation of Rift Structure along the Mid-Niger Valley, Nigeria" Journal of African Earth Sciences **1** (1983) 131. https://doi.org/10.1016/0899-5362(83)90004-0.

[27] D. E. Ajakaiye & K. A. Burke, "Bouguer gravity map of Nigeria", Tectonophysics **16** (1973) 103. https://doi.org/10.1016/0040-1951(73)90134-0.

[28] A. J. Whiteman, *Nigeria: It's Petroleum Geology: Resources and Potential*, Graham and Trotman, London, 1982, pp. 384–394. https://doi.org/10.1007/978-94-009-7361-9.

[29] S. P. Braide, "Syntectonic Fluvial Sedimentation in the Central Bida Basin", Journal of Mining and Geology **28** (1992) 55. https://www.sciepub.com/reference/108380.

[30] S. B. Ojo., "Origin of a major aeromagnetic anomaly in the Middle Niger Basin, Nigeria", Tectonophysics **185** (1990) 162. https://doi.org/10.1016/0040-1951(90)90410-A.

[31] H. A. Jones, "The Oolitic Ironstone of Agbaja Plateau, Kabba Province", Record of the Geological Survey of Nigeria **1** (1958) 20. https://www.sciepub.com/reference/110330.

[32] D. R. Adeleye & T. F. J. Dessauvagie, "Stratigraphy of the Niger Embayment, near Bida, Nigeria", in *African Geology,* T. F. J. Dessauvagie & A. J. Whiteman (Eds.), University of Ibadan Press, Ibadan, Nigeria, 1972, pp. 181–185. https://www.scirp.org/reference/referencespapers?referenceid=3159922.

[33] O. J. Ojo & S. O. Akande, "Sedimentology and depositional environments of the Maastrichtian Patti Formation, south-eastern Bida Basin, Nigeria", Cretaceous Research **30** (2009) 1425. https://doi.org/10.1016/j.cretres.2009.08.006.

[34] S. O. Akande, O. J. Ojo, B. D. Erdtmann & M. Hetenyi, "Palaeoenvironments, Organic Petrology and Rock-eval Studies on Source Rock Facies of the Lower Maastrichtian Patti Formation, Southern Bida Basin, Nigeria", Journal of African Earth Sciences **41** (2005) 406. https://doi.org/10.1016/j.jafrearsci.2005.07.006.

[35] S. R. Taylor & S. M. Mclennan, *The Continental Crust: Its Composition and Evolution: An Examination of the Geochemical Record Preserved in Sedimentary Rocks*, Blackwell Science, Oxford, U.K, 1985 pp. 1–312. https://search.worldcat.org/title/continental-crust-its-composition.

[36] H. Rollinson, *Using Geochemical Data: Evaluation, Presentation, Interpretation*, Longman, 1993, pp. 1–352. https://www.researchgate.net/profile/Mahjoor-Lone/post/.

[37] P. E. Potter, "Petrology and chemistry of modern big river sands", Journal of Geology **86** (1978) 449. https://doi.org/10.1086/649711.

[38] B. P. Roser & R. J. Korsch "Determination of tectonic setting of sandstone-mudstone suites using SiO_2 content and K_2O/Na_2O ratio", Journal of Geology **94** (1986) 650. https://www.journals.uchicago.edu/doi/abs/10.1086/629071.

[39] B. P. Roser, R. A. Cooper, S. Nathan & A. J. Tulloch, "Reconnaissance sandstone geochemistry, provenance, and tectonic setting of the lower Paleozoic terranes of the West Coast and Nelson, New Zealand: New Zealand", Journal of Geology and Geophysics **39** (1996) 16. https://doi.org/10.1080/00288306.1996.9514690.

[40] R. Cox, D. R. Lowe & R. L. Cullers, "The influence of sediment recycling and basement composition on evolution of mudrock chemistry in the southwestern United States", Geochimica et Cosmochimica Acta **59** (1995) 2940. https://doi.org/10.1016/0016-7037(95)00185-9.

[41] K. A. W. Crook, "Lithogenesis and geotectonics: the significance of compositional variation in flysch arenites (graywackes)", in *Modern and Ancient Geosynclinal Sedimentation*, R. H. Dott Jr., R. H. Shaver (Eds.), SEPM Special Publication, 1974, pp. 304–310. https://doi.org/10.2110/pec.74.19.0304.

[42] H. W. Nesbitt & G. Young, "Early Proterozoic climates and plate motions inferred from major elements chemistry of lutites", Nature **299** (1982) 717. https://doi.org/10.1038/299715a0.

[43] L. Harnois, "The CIW index: a new chemical index of weathering", Sedimentary Geology **55** (1988) 322. https://doi.org/10.1016/0037-0738(88)90137-6.

[44] C. M. Fedo, H. W. Nesbitt & G. M. Young, "Unraveling the effects of potassium metasomatism in sedimentary rocks and paleosols, with implications for paleoweathering conditions and provenance", Geology **23** (1995) 924. http://dx.doi.org/10.1130/0091-7613(1995)023%3C0921:UTEOPM%3E2.3.CO;2.

[45] C. M. Fedo, K. A. Eriksson & E. J. Krogstad, "Geochemistry of shales from the Archean (3.0 Ga) Buhwa Greenstone Belt, Zimbabwe: implications for provenance and source-area weathering", Geochimica et Cosmochimica Acta **60** (1995) 1763. https://doi.org/10.1016/0016-7037(96)00058-0.

[46] C. Descourvieres, G. Douglas, L. Leyland, N. Hartog & H. Prommer, "Geochemical reconstruction of the provenance, weathering and deposition of detrital-dominated sediments in the Perth Basin: the Cretaceous Leederville Formation, south-west Australia", Sedimentary Geology **236** (2011) 75. https://doi.org/10.1016/j.sedgeo.2010.12.006.

[47] P. J. Depetris & J. L. Probst, "Variability of the chemical index of alteration (CIA) in the Paraná River suspended load", Mineralogical Magazine **62A** (1998) 367. https://doi.org/10.1180/minmag.1998.62A.1.193.

[48] X. Long, C. Yuan, M. Sun, W. Xiao, Y. Wang, K. Cai & Y. Jiang, "Geochemistry and Nd isotopic composition of the Early Paleozoic flysch sequence in the Chinese Altai, Central 42 Asia: Evidence for a northward-derived mafic source and insight into Nd model ages in accretionary orogeny", Gondwana Research **22** 2012 554. https://doi.org/10.1016/j.gr.2011.04.009.

[49] H. W. Nesbitt & G. M. Young, "Prediction of some weathering trends of plutonic and volcanic rocks based on thermodynamic and kinetic considerations", Geochimica et Cosmochimica Acta **48** 1984 1534. https://doi.org/10.1016/0016-7037(84)90408-3.

[50] H. W. Nesbitt & G. M. Young, "Formation and diagenesis of weathering profiles", Journal of Geology **97** (1989) 147. https://doi.org/10.1086/629290.

[51] D. Garcia, M. Fonteilles & J. Moutte, "Sedimentary fractionation between Al, Ti, and Zr and genesis of strongly peraluminous granites", Journal of Geology **102** (1994) 411. https://doi.org/10.1086/629683.

[52] M. J. Le-Bas, R. W. Le Maitre, A. Streckeisen & B. Zanettin, "A chemical classification of volcanic rocks based on the total alkali-silica diagram", Journal of Petrology **27** (1986) 750. https://doi.org/10.1093/petrology/27.3.745.

[53] K. Hayashi, H. Fujisawa, H. Holland & H. Ohmoto, "Geochemistry of 1.9 Ga sedimentary rocks from northeastern Labrador, Canada", Geochimica et Cosmochimica Acta **61** (1997) 4137. https://doi.org/10.1016/S0016-7037(97)00214-7.

[54] D. J. Wronkiewicz & K. C. Condie, "Geochemistry and Mineralogy of Sediments from the Ventersdorp and Transvaal Supergroups, South Africa: Cratonic Evolution during the Early Proterozoic", Geochimica et Cosmochimica Acta **54** (1990) 354. https://doi.org/10.1016/0016-7037(90)90323-D.

[55] R. L. Cullers, "The chemical signature of source rocks in size fractions of Holocene stream sediment derived from metamorphic rocks in the wet mountains region, Colorado, USA", Chemical Geology **113** (1994) 343. https://doi.org/10.1016/0009-2541(94)90074-4.

[56] R. L. Cullers, "The geochemistry of shales, siltstones and sandstones of Pennsylvanian-Permianage, Colorado, USA: implications for provenance and metamorphic studies", Lithos **51** (2000) 181. https://doi.org/10.1016/S0024-4937(99)00063-8.

[57] K. C. Condie & D. J. Wronkiewicz, "A new look at the Archean-Proterozoic boundary: Sediments and the tectonic setting constraint", in *Precambrian Continental Crust and Its Economic Resources*, S. M. Naqvi (Ed.), Elsevier, Amsterdam, 1990, pp. 61-84. https://doi.org/10.1016/S0166-2635(08)70162-2.

[58] H. Basu, P. S. Dandele, K. Ramesh Kumar, K. K. Achar, & K. Umamaheswar, "Geochemistry of black shales from the Mesoproterozoic Srisailam Formation, Cuddapah basin, India: Implications for provenance, palaeoweathering, tectonics, and timing of Columbia breakup", Geochemistry **77** (2017) 596. https://doi.org/10.1016/j.chemer.2017.10.002.

[59] S. M. McLennan, S. Hemming, D. K. McDaniel & G. N. Hanson, "Geochemical approaches to sedimentation, provenance, and tectonics", in *Processes Controlling the Composition of Clastic Sediments*, M. J. Johnsson, A. Basu, (Eds.), Special Paper of Geological Society of America, USA, 1993, 284, pp. 40. https://doi.org/10.1130/SPE284-p21.

[60] R. L. Cullers, & J. L. Graf, "Rare Earth Elements in Igneous Rocks of the Continental Crust: Intermediate and Silicic Rocks - Ore Petrogenesis", in *Developments in Geochemistry*, P. Henderson (Ed.) Elsevier, 1984, pp. 275-316. https://doi.org/10.1016/B978-0-444-42148-7.50013-7.

[61] P. A. Floyd & B. E. Leveridge, "Tectonic environment of the Devonian Gramscatho basin, south Cornwall: framework mode and geochemical evidence from turbiditic sandstones", Journal of the Geological Society **144** (1987) 542. https://doi.org/10.1144/gsjgs.144.4.0531.

[62] R. L. Cullers, "Implications of elemental concentrations for provenance, redox conditions, and metamorphic studies of shales and limestones near Pueblo, CO, USA", Chemical Geology **191** (2002) 327. https://doi.org/10.1016/S0009-2541(02)00133-X.

[63] L. Bracciali, M. Marroni, L. Pandolfi & S. Rocchi, "Geochemistry and petrography of Western Tethys Cretaceous sedimentary covers (Corsica and Northern Apenninces): from source areas to configuration of margins", in *Sedimentary Provenance and Petrogenesis: Perspectives from Petrography and Geochemistry*, J. Arribas, S. Critelli, M. J. Johnsson (Eds.), Geological Society of America Special Paper, 2007, pp. 73–93. https://doi.org/10.1130/2006.2420(06).

[64] J. B. Maynard, R. Valloni & H. Yu, "Composition of modern deep-sea sands from arc-related basins. Geological Society of London", Special Publication **10** (1982) 551. https://doi.org/10.1144/GSL.SP.1982.010.01.36.

[65] B. P. Roser & R. J. Korsch, "Provenance signatures of sandstone-mudstone suites determined using discrimination function analysis of major-element data", Chemical Geology **67** 1988 139. https://doi.org/10.1016/0009-2541(88)90010-1.

[66] S. M. McLennan, S. R. Taylor, M. T. McCulloch & J. B. Maynard, "Geochemical and Nd-Sr isotopic composition of deep-sea turbidites: crustal evolution and plate tectonic associations", Geochimica et Cosmochica Acta **54** (1990) 2015. https://doi.org/10.1016/0016-7037(90)90269-Q.

[67] S. M. McLennan, & S. R. Taylor, "Sedimentary-Rocks and Crustal Evolution: Tectonic Setting and Secular Trends", Journal of Geology **99** (1991) 1. https://doi.org/10.1086/629470.

[68] B. D. Evamy, J. Haremboure, P. Kamerling, W. A. Knaap, F. A. Molloy & P. H. Rowlands, "Hydrocarbon habitat of Tertiary Niger Delta", American Association of Petroleum Geologists Bulletin **62** (1978) 39. http://doi.org/10.1306/C1EA47ED-16C9-11D7-8645000102C1865D.

[69] J. E. Damuth & N. Kumar, "Amazon Cone: Morphology, Sedimentation, Growth Pattern, and Comparisons with Other Modern Submarine Fan", Marine Geology **18** (1975) 117. https://doi.org/10.1016/0025-3227(75)90008-2.

[70] T. N. Zobah, C. D. Adenutsi, G. C. Amedjoe, M. C. Wilson, C. D. Boateng, J. A. Quaye, S. Erzuah, L. Wang, G. Zhao, H. Karimaie & S. K. Danuor, "A review on the provenance of the Voltaian Basin, Ghana: Implications for hydrocarbon prospectivity", Scientific African **18** (2022) e01429. https://doi.org/10.1016/j.sciaf.2022.e01429.